Axial Thermal Rotation of Slender Rods

Dichuan Li, Nikta Fakhri, Matteo Pasquali, and Sibani Lisa Biswal

Phys. Rev. Lett. **106**, 188302 — Published 3 May 2011

DOI: 10.1103/PhysRevLett.106.188302

Axial Thermal Rotation of Slender Rods

Dichuan Li, Nikta Fakhri, Matteo Pasquali, and Sibani Lisa Biswal*

Department of Chemical and Biomolecular Engineering, Rice University, Houston, Texas 77005

*Corresponding author. Email: biswal@rice.edu.

ABSTRACT

Axial rotational diffusion of rod-like polymers is important in processes like microtubule filament sliding and flagella beating. By imaging the motion of small kinks along the backbone of chains of DNA-linked colloids, we produce a direct and systematic measurement of axial rotational diffusivity of rods both in bulk solution and near a wall. The measured diffusivities decrease linearly with chain length, irrespective of distance from a wall, in agreement with slender-body hydrodynamics theory. Moreover, the presence of small kinks does not affect the chain's axial diffusivity. Our system and measurements provide insights into fundamental axial diffusion processes of slender objects, which encompass a wide range of entities including biological filaments and linear polymer chains.

17 **BODY**

18 Unlike spheres, highly anisotropic objects diffuse in a complex manner,
19 particularly so if they are flexible. The combined effects of shape anisotropy, internal
20 degrees of freedom, and environment greatly influence their behavior. Some of these
21 dynamical effects are now being understood, like the strong coupling between
22 translational diffusion and transverse rotation (usually simply termed rotation) [1] and
23 enhanced transverse rotational diffusion of slightly flexible rods in crowded
24 environments[2]. Despite its crucial importance in structuring of liquid crystals [3] and in
25 biological processes such as lipid bilayer dynamics[4] and microtubule sliding[5, 6],
26 rotational diffusion around the long axis (axial rotation) of rod-like molecules is still
27 poorly characterized and not understood. Direct measurement of axial rotation is
28 challenging because most of the electro-optical properties of cylindrical macromolecules
29 are also axisymmetric[7]. NMR relaxation[4], fluorescence anisotropy decay[8], and 3D-
30 tracking of attached quantum dots [6, 9] have been used to measure the axial rotation of
31 rod-like molecules. The first two techniques measure ensemble average properties and
32 are model dependent; the third lacks sufficient accuracy to capture diffusion.

33 Rod-like colloidal model systems [8-10] can be visualized accurately in real time
34 and space and have tunable length and stiffness. Their axial symmetry can be broken
35 simply, as shown by the recent observation of the axial rotation of a rod-like tetramer
36 along its long axis[10]. Here, we report a systematic study of axial rotational diffusivity
37 of slender rods by directly observing with high accuracy the dynamics of asymmetric
38 DNA-linked magnetic colloidal particles.

39 Axial rotational diffusion of elongated colloids was reported in 1827 by Robert

Brown in the first report on thermal (now called Brownian) motion: "oval particles … their motion consisting in turning usually on their longer axis, and then often appearing to be flattened." [11]. Brown's observation relied on the slight asymmetry of arsenic trioxide flakes. The same symmetry breaking principle is used in our experiments, but the measurements are quantitative with high precision. The colloidal rods consist of DNA-grafted paramagnetic particles aligned by a magnetic field and connected by linker DNA strands through hybridization[12, 13]. Their axial rotation is revealed by the relative motions of small kinks along their backbones, recorded by video microscopy and analyzed by image processing. The kinks act as tracers and are sufficiently large for accurate imaging while small enough not to introduce significant deviation from a perfectly straight rod in terms of axial rotational diffusivity. We first track the motion of kinks in 6 - 54μm stiff rigid rods undergoing Brownian motion near a flat substrate to measure their axial rotational diffusivities. Subsequently, we apply a magnetic field to control the distance between the rods and the substrate and measure their axial rotational diffusivities in bulk. These measured diffusivities match reasonably well with theoretical predictions [7, 14-16], confirming the validity of the slender-body hydrodynamic theory.

These rigid rods are made by linking 15-base oligonucleotides-grafted[13, 17] (surface density 5×10^4 strand/μm^2) paramagnetic polystyrene MyOne beads (Dynal Biotech, Oslo, Norway) under a uniform magnetic field[13]. Due to slight non-uniformity in the distribution of magnetic material inside the particles, their centers of mass deviate from the straight-line magnetic dipole alignment, forming kinks. These kinks are permanently set by hybridization of linker DNA and particle surface DNA. When the field is removed, the linked chains undergo quasi-2D Brownian motion near the substrate

due to confinement by gravity (Figure 1a~h and Figure 2a). To quantify the stiffness of these chains with contour length L, their persistence length, Lp is measured to be 50 ± 7 mm (L/Lp ranging from 5×10^{-5} to 10^{-3}) via Fourier mode analysis of their curvature induced by thermal fluctuations[13]. The Brownian motion of the isolated chains is recorded and the axial rotational angle, $\Phi(s_i)$, is analyzed along the chain's arclength, s, for each bond angle, i (see EPAPS for details).

For each chain near the substrate (Figure 4 bottom-left inset), we measure the transverse rotational diffusivity and compare that with theory[1] to confirm that it is not attached to the substrate (Figure S1). To measure bulk axial rotational diffusivity, we use a magnetic gradient field to levitate the rod to ~10 μm above the substrate. The chain diffuses freely along the vertical axis, indicating that vertical forces are balanced (Figure 4 top-right inset).

The distribution of bond angles between each pair of bond vectors (bond number) can be measured (Figure 3a). For example, the bond angle between the 1st and 2nd vectors (bond number 1) ranges from -5 to +5 degrees while the bond angles between the 7th and 8th vectors (bond number 7) range from -15 to +15 degrees. Since this range of angles is symmetric about 0 degrees, it indicates that the chain is making full axial rotations. We can calculate $\Phi(s_i)$ from the kinks whose bond angle exceeds 14 degrees (chosen to minimize error while still providing a statistically sufficient number of kinks within a chain). For each kink, we compute $\Phi(s_i)$ based on the geometry[18] in Figure 2b, where solid lines represent a 3D construct and dashed lines are 2D projections on the image plane. The final calculated $\Phi(s_i)$ spans between 0 and π (Figure 3b) and has a uniform distribution (Figure 3c). This indicates the rods undergo Brownian motion

without any bias in the direction of axial rotation. Mean squared displacement (MSD) of $\Phi(s_i)$ of each chosen kink within a rod is plotted against lag time Δt (Figure 3d), i.e., the time elapsed between two measurements. Finally, the axial rotational diffusivities D_{ar} are calculated by fitting a straight line to the MSD vs. lag time curve using the Einstein relation $\left\langle \left(\Phi(t+\Delta t)-\Phi(t)\right)^2 \right\rangle_t = 2D_{ar}\Delta t$. Measured diffusivities from different kinks within each rod are averaged to give the final values and standard deviations.

The drag coefficient of a rigid rod rotating around its long axis predicted by slender-body hydrodynamic theory[5, 14, 19] is approximately the sum of rotational drag coefficients of spheres, $8\pi\eta r^3$, constituting the rod, i.e.,

$$D_{ar}^{Bulk} = \frac{k_B T}{4\pi\eta r^2 L} \tag{1}$$

where k_B is Boltzmann constant, T is absolute temperature, η is the solvent viscosity, r is the bead radius, and L is the rod length.

To test the slender-body hydrodynamic theory, we measured the axial rotational diffusivities of rigid rods in bulk liquid. For each chain, a magnetic field is applied that has a gradient in the vertical direction but is uniform in the horizontal plane. The magnetic field in the horizontal plane induces dipole interactions that keep the chain from rotating in the image plane[17, 19], but does not affect the force balance in the image plane; therefore, the axial rotational diffusion of the chain should not be affected. The measured bulk axial rotational diffusivities of the 6 rigid chains (green circles in Figure 4) decrease with increasing chain length in agreement with slender-body hydrodynamic theory (red line in Figure 4).

Near a wall, diffusion is slower due to the hydrodynamic reflections of the rod on

the wall, according to [15, 20]

$$D_{ar}^{Wall} = \frac{k_B T}{4\pi\eta r^2 L}\sqrt{1-(r/h)^2} \qquad (2)$$

where h is the distance between the center of the rod (beads) and the wall. We measure the axial rotational diffusivities of rigid rods near a wall by monitoring their Brownian motion near the glass substrate. Due to the high density of the paramagnetic beads (~1800 kg/m^3), chains longer than 6 beads are confined in quasi-2D[13] and rarely fluctuate out of the focal plane (~300 nm). The data (blue circles in Figure 4) fit reasonably well Equation 2 with a power law of -1 (black line in Figure 4) in a log-log plot. The right-hand side of Equation 2 contains the same bulk diffusivity term as in Equation 1 and a factor determined by the height of the rod above the substrate. Because no systematic deviation of data points from Equation 2 is observed when using a single fitting parameter, h ($h = r + 0.12\mu m$), all the chains, long and short, have approximately the same average height above the substrate. The value of the height is in agreement with both the height of the same chains calculated using their short-axis rotational dynamics data[18] ($h = r + 0.13\mu m$, Figure S1, see Supplementary Material) and the height of more flexible chains calculated from their bending relaxation dynamics ($h = r + 0.15\mu m$)[13]. The above evidence strongly suggests the validity of previous hydrodynamic dissipation model.

To claim high precision in our axial rotational diffusivity measurement, we quantify all the major sources of error. Error (1) comes from the inaccuracy in determining the particles' centers of mass positions. A ±4 nm position error[17] would lead to $1° \sim 4°$ error in the $\Phi(s_i)$ measurement, depending on the instantaneous position

of the kink. This random error source ultimately leads to a systematic underestimate of diffusivity by up to 3%. Error (2) comes from the fact that kinks are ubiquitous in any rod we measure. Depending on the size of each kink, its effect on the deviation of the axial rotational drag coefficient of the whole chain is given by the expression $\zeta^{error} = 6\pi\eta r z^2$ [21], where z is the particle center of mass deviation from the long axis. We use the theory for straight rigid rods that does not take into account the kinks with size $2^o \le \phi(s_i) \le 20^o$, which is equivalent to an overestimate of diffusivity by 2%. Error (3) results from the fact that the $\phi(s_i)$ angles should vary between -∞ and +∞ but are only measured to be between -π/2 and π/2. This effect is equivalent to confined 1D diffusion between 2 walls[22] and would saturate the MSD vs. time curves (Figure 3d) as time approaches the axial rotational relaxation time. This effect could potentially result in an underestimate of diffusivity by $O\left(t/2\pi^2\tau\right)$. We reduce this underestimation to less than 1% by limiting the time scale plotted to be less than 5% of the relaxation time scale. As seen in Figure 3d, the MSD vs. time curves are straight within 0~5s timeframe (relaxation time 200~1000s). Error (4) is due to the assumption that both centers of mass of the particles (left and right in Figure 2b) next to the kinked particle (top one in Figure 2b) are on the rotation axis, which might not be true due to the fact that the kink arrangement within a rod is random and 3D in nature. Error (5) is caused by occasional tilting of the rods during recording that results in inaccurate particle distance measurement. Errors (4) and (5) are negligible (causing the error in the final measured diffusivity values to be <1%) since the tilting angle and the degree of axial mismatch are small enough[17, 23]. In summary, the upper bound of error is ±3%, which is unprecedented in single rod axial rotational diffusivity measurements.

In this letter we have demonstrated a convenient and systematic approach to measure axial rotational diffusivities of colloidal rigid rods of length 6~54μm, both in bulk and near a wall. We have shown that the experimentally measured diffusivities match reasonably well with slender-body hydrodynamics theory calculations. Our DNA-linked colloidal rods, with controllable length, rigidity and elevation, in conjunction with the imaging and processing technique, provide an excellent prototype to study semiflexible filament axial rotation, twisting and writhing dynamics. This opens the door to investigating polymer dynamics using colloidal rods both in bulk and confined environments.

ACKNOWLEDGEMENT

The authors gratefully thank George J. Hirasaki for insightful discussions. This work is supported in part by the Office of Naval Research YIP (Award N00014-07-1-0820), the National Science Foundation (CBET-0955003), and the Welch Foundation (Award C-1668).

REFERENCES

[1] Y. Han *et al.*, Science **314**, 626 (2006).

[2] N. Fakhri *et al.*, Science **330**, 1804 (2010).

[3] J. Leisen *et al.*, Journal of Chemical Physics **97**, 3749 (1992).

[4] R. W. Pastor, R. M. Venable, and M. Karplus, Proceedings of the National Academy of Sciences of the United States of America **88**, 892 (1991).

[5] J. Yajima, and R. A. Cross, Nature Chemical Biology **1**, 338 (2005).

[6] J. Yajima, K. Mizutani, and T. Nishizaka, Nature Structural & Molecular Biology **15**, 1119 (2008).

[7] J. G. Delatorre, and V. A. Bloomfield, Quarterly Reviews of Biophysics **14**, 81 (1981).

[8] R. L. Christensen, R. C. Drake, and D. Phillips, Journal of Physical Chemistry **90**, 5960 (1986).

[9] B. Nitzsche, F. Ruhnow, and S. Diez, Nature Nanotechnology **3**, 552 (2008).

[10] L. Hong, S. M. Anthony, and S. Granick, Langmuir **22**, 7128 (2006).

[11] R. Brown, A Brief Account of Microscopical Observations on the Particles Contained in the Pollen of Plants, in The Miscellaneous Botanical Works of Robert Brown, edited by J.J. Bennett, Vol 1, p. 487 (Robert Hardwicke, London, 1866); ark:/13960/t7tm7s378

[12] D. C. Li, J. Rogers, and S. L. Biswal, Langmuir **25**, 8944 (2009).

[13] D. C. Li, S. Banon, and S. L. Biswal, Soft Matter **6**, 4197 (2010).

[14] R. G. Cox, Journal of Fluid Mechanics **44**, 791 (1970).

[15] D. J. Jeffrey, and Y. Onishi, Quarterly Journal of Mechanics and Applied Mathematics **34**, 129 (1981).

[16] A. J. Hunt, F. Gittes, and J. Howard, Biophysical Journal **67**, 766 (1994).

[17] D. C. Li, C. N. Lam, and S. L. Biswal, Soft Matter **6**, 239 (2010).

[18] d. a. See EPAPS Document No. E-PRLTAO-96-038625 for materials and methods, and a movie showing rotational diffusion of a 12-bead rod-like chain. For more information on EPAPS, see http://www.aip.org/pubservs/epaps.html.

[19] S. L. Biswal, and A. P. Gast, Physical Review E **69**, 9 (2004).

[20] J. Howard, *Mechanics of Motor Proteins and the Cytoskeleton* (Sinauer Associates, Inc., Sunderland, Massachusetts, 2001).

[21] N. Suzuki *et al.*, Biophysical Journal **70**, 401 (1996).

[22] T. Bickel, Physica a-Statistical Mechanics and Its Applications **377**, 24 (2007).

[23] J. C. Crocker, and D. G. Grier, Journal of Colloid and Interface Science **179**, 298 (1996).

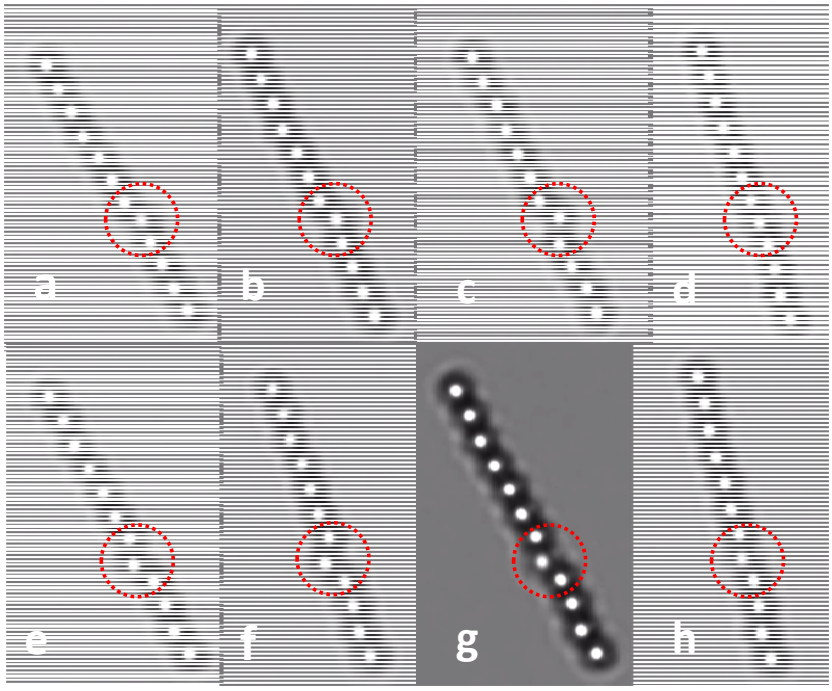

Figure 1. Snapshots of a 12-bead rigid DNA-linked chain under Brownian motion in aqueous solution near the bottom substrate. The snapshots a~h are taken 10 seconds apart and the red dashed circles are highlighting the kink formed by the 7th, 8th and 9th bead from the left. The unusual large size ($\phi \approx 75^o$) of this kink is only for demonstration whereas the kinks used to measure the axial rotational diffusivities in this letter are much smaller than this ($14^o \le \phi \le 25^o$).

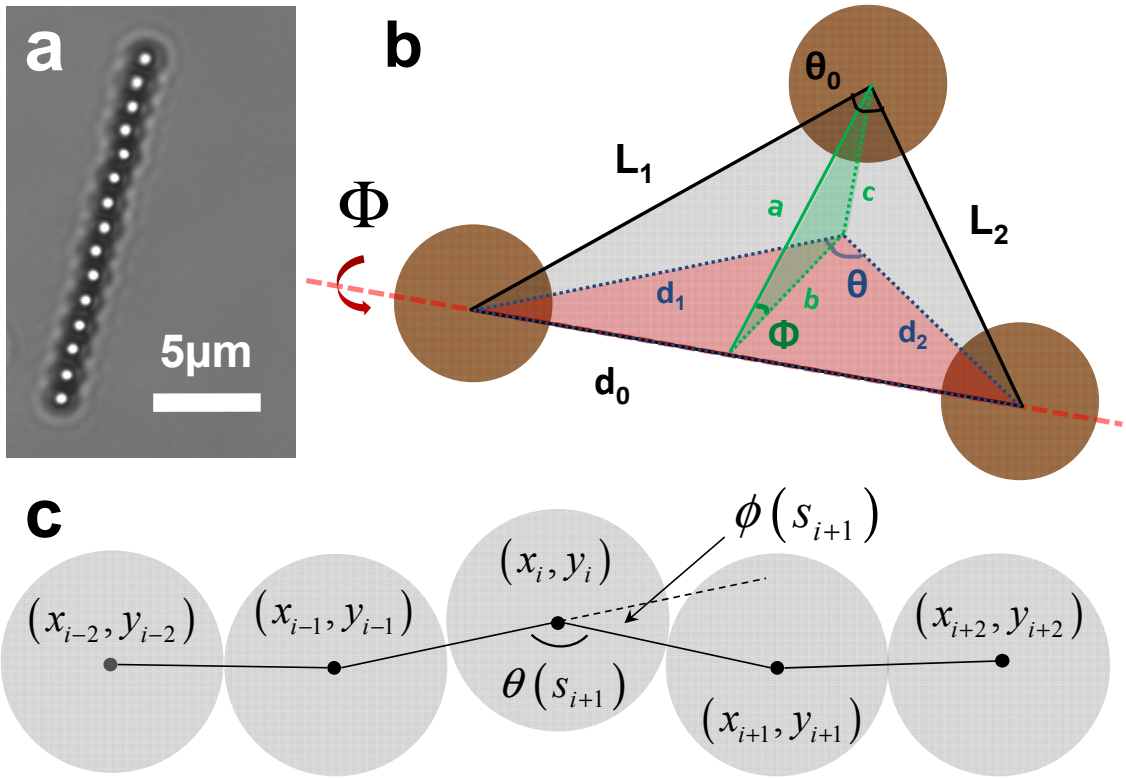

Figure 2. Measuring axial rotation of a 15-bead DNA-linked chain by tracking motions of kinks. a) Snapshot of a 15-bead DNA-linked chain undergoing Brownian motion. b) Geometry of a kink in 3D configuration and its projection. c) Definitions of position coordinates, bond angle $\phi(s_i)$ and tangent angle $\theta(s_i) = \pi - \phi(s_i)$ along the chain.

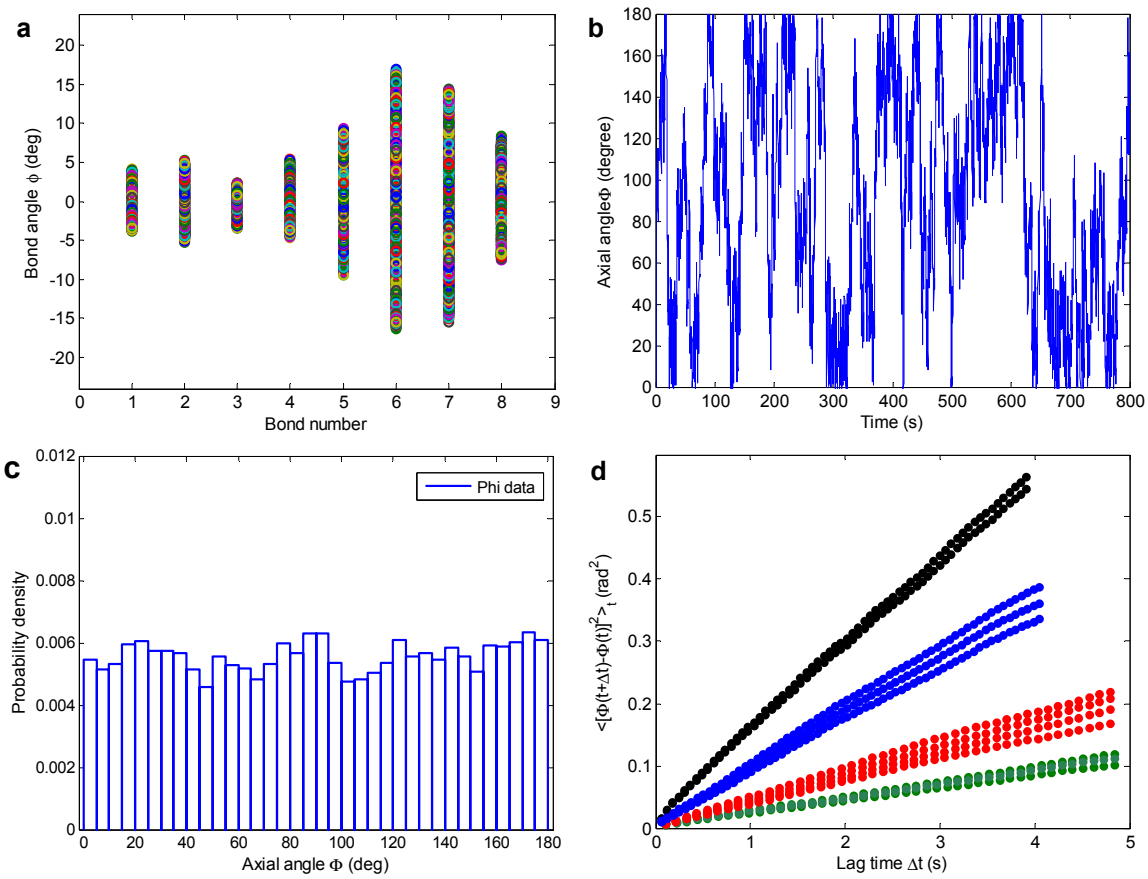

Figure 3. a) Overlay of bond angles ϕ of all kinks in a 10-bead chain within 800 seconds. b) Axial rotational angle $\Phi(t)$ measured from the sixth kink of the same chain in a). c) Histogram of the same angles in plot b). d) Typical plot of axial rotational angular mean-squared displacement (MSD) as a function lag time of 10-bead (black circle), 16-bead (blue circles), 30-bead (red circles) and 40-bead (green circles) chains in bulk.

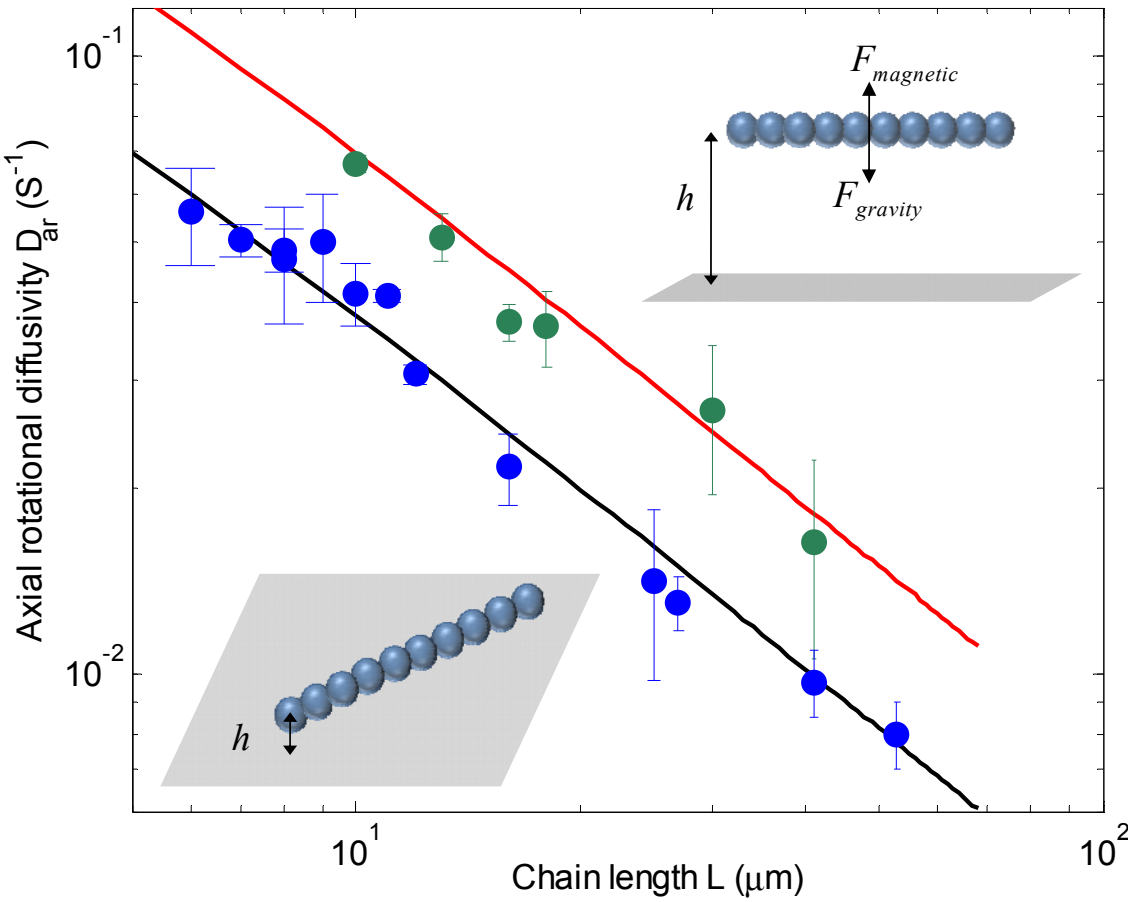

Figure 4. Axial rotational diffusivities of rigid rods. Slender-body hydrodynamics theory predictions of axial rotational diffusivitis in bulk (red line) and near a wall (black line) as a function of rod lengths. Experimental measured axial rotational diffusivities of rods in bulk (green circles) and near a wall (blue circles). Error bars are standard deviations of axial rotational diffusivities obtained from different kinks of the same chains. (*Insets*) Schematic illustrations of a chain near a wall (bottom left, where *h* is the distance between the center of the beads and the wall) and a chain elevated by a magnetic field (top right). Distances are not to scale.